Contribution from the Departments of Chemistry, University of Victoria, P.O. Box 1700, Victoria, BC, Canada V8W 2Y2, and St. Mary's University, Halifax, NS, Canada B3H 3C3

Crystal and Solution Structure of Two Dinuclear Hexadentate Macrocyclic Complexes of Palladium(II)

A. McAuley,*[†] T. W. Whitcombe,[†] and M. J. Zaworotko[‡]

Received December 28, 1990

Two dinuclear macrocyclic complexes of palladium with hexadentate ligands have been synthesized. The crystal structures of $Pd_2([18]aneN_6)Br_4 \cdot 4H_2O$ ([18]aneN$_6$ = 1,4,7,10,13,16-hexaazacyclooctadecane) ($P\bar{1}$, a = 8.092 (2) Å, b = 11.533 (2) Å, c = 7.699 (2) Å, α = 72.85 (2)°, β = 100.52 (3)°, γ = 112.20 (2)°, V = 634.3 Å^3, Z = 1, R = 0.066, R_w = 0.069) and $Pd_2([20]aneN_6)Br_4 \cdot H_2O$ ([20]aneN$_6$ = 1,4,7,11,14,17-hexaazacycloeicosane) (*Cmcm*, a = 9.375 (4) Å, b = 13.992 (5) Å, c = 18.845 (7) Å, V = 2472 Å^3, Z = 4, R = 0.041, R_w = 0.045) were determined, and the palladium ions were each found to be coordinated to three amines of the ligand and a bromine anion. The halide atoms are disposed trans and cis in the two complexes, respectively. A metal-metal distance of 3.018 Å was found in the $Pd_2([18]aneN_6)Br_2^{2+}$ cation. For both complexes, NMR spectroscopy suggests that the rigidity of the crystalline structures is maintained in solution under neutral or acidic conditions. However, fluxionality is observed in basic media. Preliminary kinetic studies demonstrate the effects of the disposition of the metal centers in the two complexes upon their ligand substitution behavior. The $Pd_2([20]aneN_6)Br_2^{2+}$ cation undergoes substitution by a mechanism similar to that observed for the $Pd_2(dien)Br^+$ analogues. For the $Pd_2([18]aneN_6)Br_2^{2+}$ cation, a dissociative mechanism may be postulated from the observed kinetics.

Introduction

Over the last few years, the importance of binuclear complexes has been increasingly recognized, especially with respect to their potential roles as homogeneous catalysts[1] as well as models for active sites in metalloproteins.[2,3] There is also a need to understand more fully the nature and extent of metal-metal interactions, particularly where there are constraints imposed by the ligand framework[4-6] which may impede or enhance metal-metal bonding. In dinuclear macrocyclic complexes, the structural integrity of the bimetallic disposition is maintained, and such complexes might be anticipated to display unique reactivity as a result of the possibility of functionally independent metal centers which are not strongly interacting. In some instances, the chelating macrocycle may rearrange to adapt to the incorporation of the metallic centers.[5] In this paper, we describe such an observation where changes in the M-M distance are related to the geometry of the complex and where there exists the possibility for the incorporation of additional anionic reagents.

The hexadentate polyazamacrocycles, illustrated by I, represent a series of ligands that may coordinate either one or two metal ions, dependent, in part, on the metal ion and on the length of

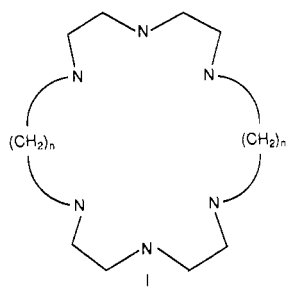

I

n = 2 : [18]aneN$_6$
n = 3 : [20]aneN$_6$

the bridging groups. In the case of the macrocycle 1,4,7,10,13,16-hexaazacyclooctadecane ([18]aneN$_6$, X = Y = $-(CH_2)_n-$, n = 2), which is the nitrogen analogue of 18-crown-6, octahedral mononuclear complexes are formed with some first-row transition metals (Ni(II),[7] Co(III),[8] Cr(III)[9]). Similar octahedral MN_6 chromophores are formed by the homologous [20]aneN$_6$ (n = 3) with Ni(II)[10] and Co(III).[11] However, with larger rings (e.g., n = 5), the corresponding Cu(II) species are dinuclear[12] and form adducts with molecular oxygen.[13] Carbonyl adducts of the dicopper(I) complex react with O_2 in the catalytic oxidation of phenol to catechol. The $Cu_2([24]aneN_6)Br_4$ complex has been shown recently[14] to exhibit five-coordination about the metal center. With elements of the second row, specifically rhodium, a number of dinuclear complexes[5,6] of larger macrocycles have been obtained with bridging and nonbridging ligands. In all of the dinuclear complexes, hexaazamacrocyclic ligands of this type may be viewed as two linked diethylenetriamine (dien) units where control of the metal-metal distance is achieved by variation of the length of the bridges.

As part of an ongoing investigation of the properties of palladium macrocycles, we have synthesized binuclear Pd(II) complexes of both [18]aneN$_6$ and [20]andN$_6$. In contrast to the species formed on reaction with triazacyclononane, $Pd([9]aneN_3)_2^{2+}$, which readily undergoes oxidation to a very stable palladium(III) ion,[15] there is no tendency toward oxidation to the d^7 ion in the dinuclear complexes. Since the palladium ions are formally d^8, no specific bonding between the metal centers is anticipated, but, like other cofacial systems, weak interaction is possible. Ligand geometry does result in a cofacial dimer where unusual metal-metal distances are observed, which are described herein.

Experimental Section

Preparation of Compounds. $[Pd_2([18]aneN_6)Br_2]Br_2 \cdot 4H_2O$. The ligand, $([18]aneN_6) \cdot 3H_2SO_4$, available from Aldrich Chemicals, was used without further purification. $([18]aneN_6) \cdot 3H_2SO_4$ (0.50 g; 0.9 mmol) was dissolved in deionized water (10 mL), and the pH was adjusted to ≈10 with NaOH. The solution was stirred at low heat and $PdCl_2$ added (0.35 g; 2.0 mmol; 2.2:1 $PdCl_2$:ligand). The solution was allowed to react for approximately 3 h, during which time it turned yellow, giving the species $[Pd_2([18]aneN_6)Cl_2](PdCl_4) \cdot H_2O$, which may be isolated. Anal. Calc: C, 17.83; H, 3.99; N, 10.40. Found: C, 17.99; H, 3.93; N, 10.33. The bromide salt was obtained by the addition of a saturated solution of

[†] University of Victoria.
[‡] St. Mary's University.

(1) (a) Maugh, T. H. *Science* **1983**, *220*, 592. (b) Roundhill, D. M.; Gray, H. B.; Che, C.-M. *Acc. Chem. Res.* **1989**, *22*, 55.
(2) Maverick, A. W.; Klavetter, J. E. *Inorg. Chem.* **1984**, *23*, 4130.
(3) Nelson, S. M. *Inorg. Chim. Acta* **1982**, *62*, 39.
(4) Lehn, J.-M. *Pure Appl. Chem.* **1980**, *52*, 2441.
(5) Lecomte, J.-P.; Lehn, J.-M.; Parker, D.; Guilheim, J.; Pascard, C. *J. Chem. Soc., Chem. Commun.* **1983**, 296.
(6) Parker, D. *J. Chem. Soc., Chem. Commun.* **1985**, 1129.
(7) Hay, R. W.; Jeragh, B.; Lincoln, S. F.; Searle, G. H. *Inorg. Nucl. Chem. Lett.* **1978**, *14*, 435.
(8) Yoshikawa, Y. *Chem. Lett.* **1978**, 109.
(9) Fortier, D. G.; McAuley, A.; Chandrasekhar, S. Unpublished results.
(10) Margulis, T. N.; Zompa, L. J. *J. Chem. Soc., Chem. Commun.* **1979**, 430.
(11) Searle, G. H.; Angley, M. E. *Inorg. Chim. Acta* **1981**, *49*, 185.
(12) Comarmond, J.; Plumeré, P.; Lehn, J.-M.; Agnus, Y.; Louis, R.; Weiss, R.; Kahn, O.; Morgenstern-Badarau, I. *J. Am. Chem. Soc.* **1982**, *104*, 6330.
(13) Bulkowski, J. E. U.S. Patent No. 659,396.
(14) Schaber, P. M.; Fettinger, J. C.; Churchill, M. R.; Nalewajek, D.; Fries, K. *Inorg. Chem.* **1988**, *27*, 1641.
(15) McAuley, A.; Whitcombe, T. W. *Inorg. Chem.* **1988**, *27*, 3090.

0020-1669/91/1330-3513$02.50/0

Table I. Crystallographic Data

(a) $Pd_2([18]aneN_6)Br_4 \cdot 4H_2O$

formula: $C_{12}H_{38}N_6O_4Br_4Pd_2$	$V = 634.4$ Å^3
fw 862.9	$Z = 1$
space group $P\bar{1}$ (No. 2)	$\rho_{obsd} = 2.18$ (2) g/cm^3
$a = 8.092$ (2) Å	$\rho_{calcd} = 2.259$ g/cm^3
$b = 11.533$ (2) Å	$\lambda = 0.71069$ Å (Mo Kα)
$c = 7.699$ (2) Å	$\mu = 80.88$ cm^{-1}
$\alpha = 72.85$ (2)°	transm coeff = 0.266–0.395
$\beta = 100.52$ (3)°	$T = 22 \pm 2$ °C
$\gamma = 112.20$ (2)°	$R(F_o) = 0.066$
	$R_w(F_o) = 0.069$

(b) $Pd_2([20]aneN_6)Br_4 \cdot H_2O$

formula: $C_{14}H_{36}N_6OBr_4Pd_2$	$V = 2472.0$ Å^3
fw 836.9	$\rho_{obsd} = 2.20$ (1) g/cm^3
space group *Cmcm* (No. 63)	$\rho_{calcd} = 2.248$ g/cm^3
$a = 9.375$ (4) Å	$\lambda = 0.71069$ (Mo Kα)
$b = 13.992$ (5) Å	$\mu = 76.9$ cm^{-1}
$c = 18.845$ (7) Å	transm coeff = 0.432–0.560
$Z = 4$	$T = 22 \pm 2$ °C
	$R(F_o) = 0.041$
	$R_w(F_o) = 0.045$

NaBr giving yellow crystals. Anal. Calc: C, 16.70; H, 4.44; N, 9.74. Found: C, 16.66; H, 4.38; N, 9.66. The overall yield is only ≈20% due to loss of Pd^{2+} in the basic media and the appearance of a second dark orange species, which has not been characterized fully.

$[Pd_2([20]aneN_6)Br_2]Br_2 \cdot H_2O$. The ligand is obtained as a minor product in the synthesis of 1,4,7-triazacyclodecane ([10]aneN$_3$) and can be isolated by column chromatography. This finding is similar to that reported[14] recently where, in the synthesis of [12]aneN$_3$, a byproduct isolated was the macrocycle [24]aneN$_6$. In addition, a new synthetic route to this ligand has been devised and will be published elsewhere.[16b] Other synthetic routes to this ligand have recently been reported.[16a] [20]aneN$_6$·6HCl (0.5 g; 1.0 mmol) was dissolved in deionized water (10 mL), and the pH was adjusted to ≈10 by using NaOH. The solution was stirred at low heat, and solid $PdCl_2$ was added (0.37 g; 2.1 mmol; 2.1:1 $PdCl_2$:ligand). After approximately 3 h, the solution turned a lemon yellow color, yielding the intermediate species $[Pd_2([20]aneN_6)Cl_2](PdCl_4)$, which was not isolated. The bromide salt was obtained upon addition of a saturated solution of NaBr giving yellow crystals. Anal. Calc: C, 20.09; H, 4.34; N, 10.04. Found: C, 20.32; H, 4.27; N, 9.77. The overall yield was ≈25% due to the reason given above, and a second orange-red species was obtained.

Spectroscopy. UV/visible spectra were obtained on either a Unicam SP8-400 or a Perkin-Elmer Lambda 4B spectrometer. ^{1}H and ^{13}C NMR spectra were obtained on either a Bruker WM250 (1-dimensional) or a Bruker AM400 (2-dimensional) NMR spectrometer. D_2O was used as the solvent and lock. Simulated NMR spectra were calculated by using a locally modified[17] version of UEAITR[18] and NMRPLOT[19] on an IBM 3083 computer with a Tektronix 4013 graphics terminal. Infrared spectra were recorded on a Perkin-Elmer 283 infrared spectrophotometer. Microanalyses were performed by Canadian Microanalytical Services, Vancouver, BC.

Crystal Data. $[Pd_2([18]aneN_6)Br_2]Br_2 \cdot 4H_2O$. Crystals were obtained by the slow evaporation of a bromide-containing solution of the compound. The crystal was mounted in a Lindemann tube with epoxy resin and photographed by Weissenberg and precession cameras. The unit cell was obtained from the least-squares refinement of the angular settings for 15 pairs of reflections accurately centered in the 2θ range 20–45°. The intensity measurements were obtained by scanning in the $\theta/2\theta$ mode, with the use of a Picker four-circle diffractometer, with 120 steps of 0.01° in 2θ counting for 0.25 s per step. Background counting was introduced for 15 s at each end of the scan. Pertinent crystallographic data are included in Table I. Three standards were collected before every 50 reflections, and no significant decrease in intensity was observed during data collection. The structure was solved for the heavy atoms by MULTAN[21] and refined by a least-squares technique using SHELX[22] to a final conventional $R = 0.066$ ($R_w = 0.069$). The atomic scattering factors were obtained from the compilation of Cromer and Mann.[23] The real and imaginary components of the anomalous dispersion were obtained from the tables compiled by Cromer and Libermann.[24]

The molecule is centered around a point of inversion, and thus, the asymmetric unit consists of half the molecule. A total of 140 parameters were necessary to define the structure with all of the atoms, except the hydrogens, being refined anisotropically. Only the hydrogen atoms for the water molecules were included in the final stages of refinement with fixed distances relative to the oxygen atom and to each other. All attempts at the inclusion of the remaining "hydrogen atoms" from the residual difference maps resulted in unrealistic bond lengths and angles. Calculation of the atomic positions of the hydrogens using SHELX was not feasible with this structure due to symmetry considerations. A consequence of this is that nine peaks remained in the residual difference map with significant electron density (>1.0 e/Å^3). The largest of these peaks, however, were located around the palladium atom.

$[Pd_2([20]aneN_6)Br_2]Br_2 \cdot H_2O$. Methods similar to those for $[Pd_2([18]aneN_6)Br_2]Br_2 \cdot 4H_2O$ were used, with the relevant changes listed in Table I. The structure was refined by a least-squares technique to a final conventional $R = 0.041$ ($R_w = 0.045$).

The molecule lies around an *mm* position within the unit cell, and therefore, possesses two crystallographically imposed mirror planes; hence, the asymmetric unit is one quarter of the molecule. Following anisotropic refinement of all non-hydrogen atoms (except one of the nitrogen atoms and the oxygen atom of the water molecule), the hydrogen atoms were locatable via inspection of the Fourier difference map and were therefore included in the final refinement stages with a common isotropic thermal parameter. The final Fourier map contained no peaks in excess of 1.0 e/Å^3, the largest of which were located around the palladium atom. The structure was also refined in the non/centrosymmetric space group *Cmc*2, but the values of R and R_w were observed to be higher and the number of correlations greater than those obtained from *Cmcm*.

Results and Discussion

Synthesis. The complexes may be prepared from aqueous solution by the addition of $PdCl_2$ to a basic solution of the ligand. Heating results in the generation of a yellow, water-soluble species, which has been isolated for the $Pd_2([18]aneN_6)$ complex and determined to be $[Pd_2([18]aneN_6)Cl_2](PdCl_4)$ (infrared: Pd–Cl at 308, 283 cm^{-1}). Solutions of these complexes are susceptible to substitution by bromide, yielding crystals of the bromide salts, $[Pd_2([18]aneN_6)Br_2]Br_2 \cdot 4H_2O$ and $[Pd_2([20]aneN_6)Br_2]Br_2 \cdot H_2O$. In each system, a second species remains in solution and may be precipitated by concentration of the filtrate. This complex has been tentatively assigned the formula $[Pd_2(\text{ligand})Br_2](PdBr_4)$, by analogy with the chloride complex. However, consistent microanalytical results for this compound have not been obtained, with the results tending to be lower than required in measured bromide and suggestive of a formulation with five bromides per dimeric cation. A final product may be isolated from the filtrate by addition of a saturated solution of sodium iodide. This compound is almost black having strong absorptions at 650, 530, and 445 nm ($\epsilon > 10^3$ M^{-1} cm^{-1}) and a shoulder at 360 nm on the charge-transfer band centered near 300 nm. The microanalytical results for the [18]aneN$_6$ species are consistent with the formulation $Pd_2([18]aneN_6)I_5$. Anal. Calc: C, 13.03; H, 2.73; N, 7.60. Found: C, 13.24; H, 2.84; N, 7.64.

No evidence for ESR activity was obtained in any of these compounds. This is consistent with the absence of compounds in nonformal oxidation states despite recent evidence[15] of the formation of stable Pd(III) complexes with macrocyclic ligands. Several large single crystals of $Pd_2([18]aneN_6)Br_4 \cdot 4H_2O$ were submitted to γ-irradiation in an attempt to generate an ESR-active species either in a single cation or as a delocalized electron through a short-chain oligomer. Despite repeated attempts, no single-electron-oxidation or -reduction products were detectable by ESR spectroscopy.

Attempts to facilitate the oxidative addition of small molecules across the Pd–Pd dinuclear unit have not succeeded. Similarly,

(16) (a) Martin, A. E.; Bulkowski, J. E. *J. Org. Chem.* **1982**, 415. (b) Fortier, D. Unpublished observations.
(17) Dixon, K. R. Private communication.
(18) Johannsen, R. B.; Ferreti, J. A.; Harris, R. K. *J. Magn. Reson.* **1970**, *3*, 84.
(19) Swalen, J. D. In *Computer Programs for Chemistry*; Detar, D. F., Ed.; W. A. Benjamin: New York, 1968; Vol. 1.
(20) P. Coppens, L. Lieserowitz, and D. Rabinovich (modified by G. W. Bushnell, University of Victoria).
(21) MULTAN: P. Main, University of New York, U.K., 1978.
(22) SHELX76, a Program for Crystal Structure Refinement: G. M. Sheldrick, University of Cambridge, U.K., 1976.
(23) Cromer, D. T.; Mann, J. B. *Acta Crystallogr., Sect. A* **1968**, *A24*, 321.
(24) Cromer, D. T.; Libermann, D. A. *J. Chem. Phys.* **1970**, *53*, 1891.

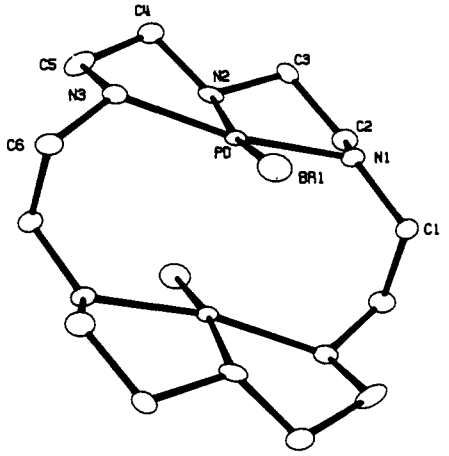

Figure 1. ORTEP view of the $Pd_2([18]aneN_6)Br_2^{2+}$ cation. Selected bond distances (Å): Pd–Br(1) = 2.395 (2), Pd–N(1) = 2.166 (10), Pd–N(2) = 1.996 (9), Pd–N(3) = 2.174 (10), Pd···Pd = 3.018 (2).

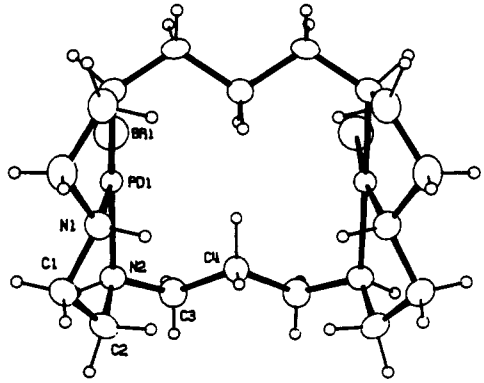

Figure 2. ORTEP view of the $Pd_2([20]aneN_6)Br_2^{2+}$ cation. Selected bond distances (Å): Pd–Br(1) = 2.429 (1), Pd–N(1) = 2.005 (6), Pd–N(2) = 2.065 (5), Pd···Pd = 5.039 (2).

Table II. Fractional Atomic Coordinates and Temperature Parameters for $Pd_2([18]aneN_6)Br_2^{2+}$ [a]

atom	*x/a*	*y/b*	*z/c*	U_{eq}, Å^2
Pd	57745 (11)	14190 (7)	90194 (11)	194 (3)
Br(1)	68608 (20)	4571 (13)	72522 (19)	443 (6)
Br(2)	33563 (24)	32599 (16)	33336 (23)	591 (7)
N(1)	3398 (13)	1332 (8)	7431 (12)	26 (4)
N(2)	5154 (13)	2547 (8)	10166 (13)	28 (4)
N(3)	8154 (13)	1937 (9)	10580 (13)	27 (4)
C(1)	2110 (17)	139 (11)	6898 (16)	33 (5)
C(2)	2460 (17)	1955 (12)	8183 (17)	34 (5)
C(3)	3880 (17)	3098 (11)	8820 (15)	29 (4)
C(4)	6845 (17)	3489 (11)	10677 (18)	34 (5)
C(5)	8037 (18)	2721 (12)	11775 (20)	40 (6)
C(6)	9000 (16)	942 (12)	11653 (18)	35 (5)
O(1)	21 (14)	6004 (10)	2408 (14)	52 (4)
O(2)	2650 (13)	5258 (10)	5020 (14)	53 (4)

[a] Estimated standard deviations are given in parentheses. Coordinates are $\times 10^n$ where n = 5, 5, 4, 4, 4 for Pd, Br, O, N, C. Temperature parameters are $\times 10^n$ where n = 4, 4, 3, 3, 3 for Pd, Br, O, N, C. U_{eq} is the equivalent isotropic temperature parameter.

attempts to oxidize or reduce these compounds electrochemically have not provided any significant results. This is due, in part, to the insolubility of these complexes in most common solvents (i.e. ethanol, acetonitrile, tetrahydrofuran, dichloromethane, chloroform, etc.). Solvated species could only be generated in H_2O and dimethyl sulfoxide (DMSO), limiting the possible reactions.

Crystal Structures. The crystal structures of the $Pd_2([18]aneN_6)Br_2^{2+}$ and $Pd_2([20]aneN_6)Br_2^{2+}$ ions are shown in Figures 1 and 2, respectively, together with the atomic labeling scheme employed. Fractional coordinates, bond lengths, bond angles, and

Table III. Interatomic Distances (Å) for $Pd_2([18]aneN_6)Br_2^{2+}$ [a]

Br(1)–Pd	2.395 (2)	C(3)–N(2)	1.544 (15)
N(1)–Pd	2.166 (10)	C(4)–N(2)	1.530 (16)
N(2)–Pd	1.996 (9)	C(5)–N(3)	1.514 (15)
N(3)–Pd	2.174 (10)	C(6)–N(3)	1.519 (15)
Pd–Pd	3.018 (1)	C(3)–C(2)	1.598 (17)
C(1)–N(1)	1.560 (15)	C(5)–C(4)	1.545 (18)
C(2)–N(1)	1.464 (15)		

[a] Estimated standard deviations are given in parentheses.

Table IV. Bond Angles (deg) for $Pd_2([18]aneN_6)Br_2^{2+}$ [a]

N(1)–Pd–Br(1)	92.2 (2)	C(4)–N(2)–Pd	109.8 (7)
N(2)–Pd–Br(1)	168.8 (3)	C(4)–N(2)–C(3)	118.7 (7)
N(2)–Pd–N(1)	88.6 (4)	C(5)–N(3)–Pd	113.0 (7)
N(3)–Pd–Br(1)	97.3 (2)	C(6)–N(3)–Pd	121.8 (7)
N(3)–Pd–N(1)	167.1 (3)	C(6)–N(3)–C(5)	107.8 (10)
N(3)–Pd–N(2)	80.4 (4)	C(3)–C(2)–N(1)	108.9 (10)
C(1)–N(1)–Pd	127.2 (7)	C(2)–C(3)–N(2)	109.2 (9)
C(2)–N(1)–Pd	104.6 (7)	C(5)–C(4)–N(2)	109.0 (9)
C(2)–N(1)–C(1)	112.2 (9)	C(4)–C(5)–N(3)	102.3 (10)
C(3)–N(2)–Pd	109.8 (7)		

[a] Estimated standard deviations are given in parentheses.

Table V. Selected Intermolecular Distances (Å) for $Pd_2([18]aneN_6)Br_2^{2+}$ [a]

atoms	dist	sym	T_x	T_y	T_z
Br(1)···Pd	3.451	−1	1	0	2
N(1)···Pd	3.724	−1	1	0	2
N(2)···Pd	4.217	−1	1	0	2
N(3)···Pd	4.018	−1	1	0	2
O(1)···Pd	3.654	−1	1	1	1
O(2)···Pd	4.039	−1	1	1	1
Br(1)···Br(1)	4.540	−1	1	0	1
Br(2)···Br(1)	4.384	−1	1	0	1
N(2)···Br(1)	3.348	−1	1	0	2
O(1)···Br(1)	4.067	−1	1	1	1
N(2)···Br(2)	3.417	1	0	0	1
O(2)···Br(2)	3.421	−1	1	1	1
N(3)···N(1)	3.424	−1	1	0	2
O(1)···N(3)	2.855	−1	1	1	1
O(2)···O(1)	2.775	−1	0	1	1

[a] The symmetry positions are for the second atom. A negative symmetry position denotes inversion. The translations (T) are applied finally.

Table VI. Fractional Atomic Coordinates and Temperature Parameters for $Pd_2([20]aneN_6)Br_2^{2+}$ [a]

atom	*x/a*	*y/b*	*z/c*	U_{eq}, Å^2
Pd(1)	0	44995 (4)	61628 (3)	212 (2)
Br(1)	0	62353 (6)	61492 (5)	467 (3)
Br(2)	50000	50000	50000	458 (4)
Br(3)	50000	31441 (9)	25000	432 (4)
N(1)	0	3077 (4)	6039 (3)	29 (2)
N(2)	2192 (5)	4354 (3)	6178 (2)	30 (1)
C(1)	1354 (6)	2832 (4)	5683 (3)	37 (2)
C(2)	2520 (7)	3308 (4)	6087 (3)	37 (2)
C(3)	2883 (6)	4767 (4)	6827 (3)	36 (2)
C(4)	2099 (8)	4502 (6)	7500 (0)	34 (3)
O(1)	0 (0)	2226 (10)	2500 (0)	96 (4)′

[a] Estimated standard deviations are given in parentheses. Coordinates are $\times 10^n$ where n = 5, 5, 4, 4, 4 for Pd, Br, O, N, C. Temperature parameters are $\times 10^n$ where n = 4, 4, 3, 3, 3 for Pd, Br, O, N, C. U_{eq} is the equivalent isotropic temperature parameter. The primed value indicates that U_{iso} is given.

Table VII. Interatomic Distances (Å) for $Pd_2([20]aneN_6)Br_2^{2+}$ [a]

Br(1)–Pd	2.429 (1)	C(2)–N(2)	1.504 (11)
N(1)–Pd	2.000 (8)	C(3)–N(2)	1.493 (11)
N(2)–Pd	2.061 (6)	C(2)–C(1)	1.494 (12)
C(1)–N(1)	1.480 (9)	C(4)–C(3)	1.510 (10)

[a] Estimated standard deviations are given in parentheses.

Table VIII. Bond Angles (deg) for $Pd_2([20]aneN_6)Br_2^{2+}$ [a]

N(1)-Pd-Br(1)	173.2 (3)	C(3)-N(2)-C(2)	112.8 (6)
N(2)-Pd-Br(1)	95.5 (2)	C(2)-C(1)-N(1)	106.5 (6)
N(2)-Pd-N(1)	84.7 (2)	C(1)-N(1)-C(1)	117.9 (8)
C(1)-N(1)-Pd	106.1 (5)	C(1)-C(2)-N(2)	110.2 (7)
C(2)-N(2)-Pd	107.1 (5)	C(4)-C(3)-N(2)	111.5 (7)
C(3)-N(2)-Pd	114.4 (5)	C(3)-C(4)-C(3)	113.5 (10)

[a] Estimated standard deviations are given in parentheses.

Table IX. Selected Intermolecular Distances (Å) for $Pd_2([20]aneN_6)Br_2^{2+}$ [a]

atoms	dist	sym	T_x	T_y	T_z
Pd(1)···Pd(1)	4.602	-1	0	1	1
Br(1)···Pd(1)	4.478	-1	0	1	1
Pd(1)···Pd(1)	5.039	-2	0	0	2
Br(3)···Pd(1)	4.473	-1	1	1	1
N(1)···Br(1)	4.234	-1	0	1	1
O···Br(1)	3.338	-1	0	1	1
N(1)···Br(3)	3.224	-1	1	1	1

[a] The symmetry positions are for the second atom. They are defined as follows (*C*-centered):

$$x, y, z \rightarrow -x, -y, -z$$

$$-x, -y, \frac{1}{2} + z \rightarrow x, y, \frac{1}{2} - z$$

$$-x, y, \frac{1}{2} - z \rightarrow x, -y, \frac{1}{2} + z$$

$$x, -y, -z \rightarrow -x, y, z$$

A negative symmetry position denotes inversion. The transitions (T) are applied finally.

important intermolecular contacts are given in Tables II–V and Tables VI–IX for $[Pd_2([18]aneN_6)Br_2]Br_2 \cdot 4H_2O$ and $[Pd_2([20]aneN_6)Br_2]Br_2 \cdot H_2O$. All other tables have been included as supplementary material.

Each macrocyclic ligand coordinates two palladium ions. The ligand may be considered as acting as two tridentate ligands that are structurally similar to substituted diethylenetriamine (dien) moieties. Thus, each complex contains two Pd(dien)X subunits linked by an aliphatic bridge that are oriented trans with respect to the Pd–Pd vector in $Pd_2([18]aneN_6)Br_2^{2+}$ and cis in $Pd_2([20]aneN_6)Br_2^{2+}$. This geometrical feature is a result of the even and odd number of methylene groups in the bridge for the [18]aneN$_6$ and [20]aneN$_6$ complexes, respectively. It is of interest to note that both van der Waals repulsion and intramolecular N–H···Br hydrogen bonding would favor the trans configuration in both complexes.

$Pd_2([18]aneN_6)Br_4 \cdot 4H_2O$. The asymmetric unit consists of half of the molecule, as the molecule is situated on a center of inversion. This, by necessity, results in the two Pd(dien)X units being parallel with each other and being in the trans configuration. The present structure is in contrast with the known structures for dinuclear complexes of larger macrocyclic ligands where the metal–dien moieties are in the plane of the ligand[5,6] and where tetranuclear complexes are possible.[25] Bulkowski[13] has also tentatively assigned an in-plane coordination geometry to carbonyl-bridged dicopper complexes of the [18]aneN$_6$ and [20]aneN$_6$ ligands.

The structure may be viewed as a consequence of a combination of two factors resulting from both the ligand and the metal. The d^8 palladium(II) ion favors square-planar geometry owing to crystal field stabilization energy. Formation of an in-plane complex within the macrocyclic cavity would require that the coordinated halides overlap, giving either a singly or doubly bridged core. The latter would better balance charge but would yield a five-coordinate metal center. While similar bridging complexes are known for palladium, their occurrence is not widespread for amine ligand systems.[26]

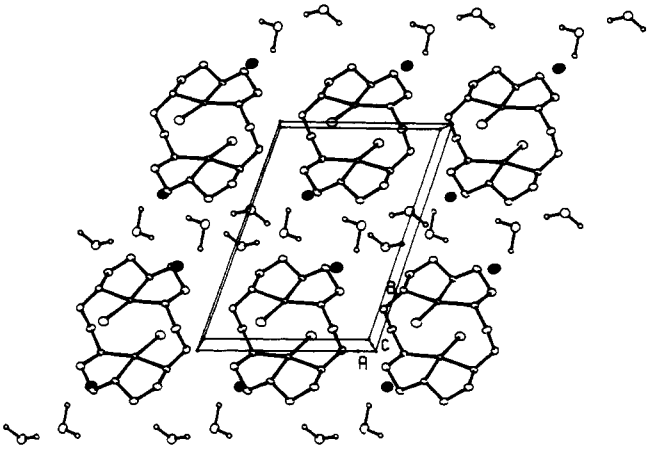

Figure 3. Cell packing diagram for the [18]aneN$_6$ complex, showing the stacking along the *a* axis and the channel-type interaction between Br(2) and lattice H_2O molecules. The noncoordinating bromide ions have been darkened for clarification.

The smaller ligand, [18]aneN$_6$, forces the close interaction of the two metal centers and, thus, inhibits the in-plane coordination of both palladium ions unless a bridging group is present. In addition, all of the nitrogens exist as sp^3 hybrids, which, if all of the nitrogens are coplanar, results in the alternation of the direction of the lone pairs around the ligand (half pointing up; half pointing down). A planar geometry for the ligand cannot provide for a consistent direction of the lone pairs, diminishing the extent of bonding possible. Indeed, the strain to maintain planarity of the lone pairs for just the "dien" fragment is observable in the bond and torsion angles for the chelating rings.

There is some evidence for hydrogen-bonding interactions in the crystalline lattice. The water molecule (O(2)) is hydrogen-bonded to the anionic bromide (Br(2)). The result of this interaction is the formation of a type of channel in the crystal between the dimeric units, which are noninteracting (Figure 3). Within the $Pd_2([18]aneN_6)Br_2^{2+}$ cation, the N(2))···Br(1) distance is 3.348 Å (see Figure 1 and Table V), indicative of a very weak H-bond.[27] This is observable from the slight shift in the N–H stretching frequencies in the infrared spectrum of $Pd_2([18]aneN_6)Br_2^{2+}$ when compared to the N–H stretch for $Pd_2([20]aneN_6)Br_2^{2+}$. However, since none of the hydrogen atoms attached to the nitrogen atoms were locatable from the Fourier difference maps, the exact position of the hydrogen and the linearity of the N–H···Br interaction is not known.

$Pd_2([20]aneN_6)Br_4 \cdot H_2O$. The asymmetric unit consists of one quarter of the cation and half of the noncoordinated anions, which means that the two Pd(dien)X moieties are not constrained to be parallel. The palladium is coordinated within the dien moiety rather than with an asymmetric but less strained 1,3-propanediyl–ethylene–triamine unit. This serves to increase the metal–metal distances and, hence, decrease any interactions between the two metal centers. With the increased size of the macrocycle, the cavity defined by the planar arrangement of the six nitrogens is larger than that for the [18]aneN$_6$ ligand. However, the molecule still adopts a structure with the PdN_3X planes approximately parallel and orthogonal to the Pd–Pd vector. The three methylene groups in the linking bridges between the two Pd(dien)Br units necessitates that the coordinated bromides are cis with respect to each other.

Since the cis geometry requires both bromide ions on the same side of the molecule, there is no possibility of hydrogen bonding internally to any of the nitrogen protons. Interaction between the adjacent bromide ions is also unlikely, as the distance between the two atoms is greater than 5 Å, which is significantly longer than the sum of their van der Waals radii.

(25) Johnson, J. M.; Bulkowski, J. E.; Rheingold, A. L.; Gates, B. C. *Inorg. Chem.* **1987**, *26*, 2644.

(26) Hartley, F. R. *The Chemistry of Platinum and Palladium*; Applied Science Publishers: London, 1973.

(27) Cotton, F. A.; Wilkinson, G. *Advanced Inorganic Chemistry*; John Wiley and Sons: New York, 1980; p 219.

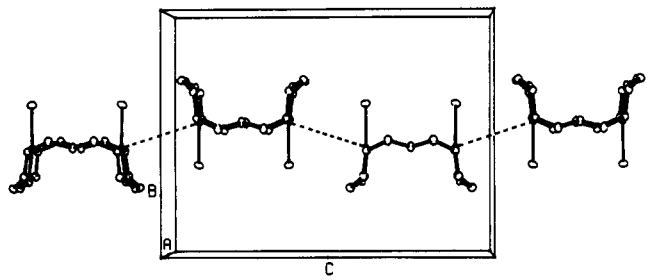

Figure 4. Cell packing diagram for the [20]aneN$_6$ cation, showing the stacking along the *c* axis and interactions between adjacent dimeric units (Pd···Pd = 4.601 (2) Å).

Metal–Metal Interactions. Throughout the above discussion of the overall crystallographic features, the question of the metal–metal distance and the extent of interaction has not been addressed. For the $Pd_2([20]aneN_6)Br_2^{2+}$ cation, an intramolecular distance of 5.039 Å is observed between palladium atoms. However, a short interionic distance of 4.602 Å is observed between palladiums in adjacent dimeric units within the unit cell, resulting from the stacking of the cations along the *c* axis as illustrated in Figure 4. The internal Pd–Pd distance in $Pd_2([18]aneN_6)Br_2^{2+}$ is considerably shorter at 3.018 (1) Å, although still somewhat longer than the value normally accepted as indicative of a Pd–Pd bond (2.751 Å in Pd metal).[28] Since both palladium atoms are in the +2 oxidation state, metal–metal interaction should result in a nonbonding overlap. Shorter distances (e.g. ≈2.5 Å)[29] have been observed for Pd(II) dimers and have been interpreted as nonbonding, but Gray et al.[1b,30] have suggested that orbital involvement may lead to a small positive interaction in cofacial d^8–d^8 systems.

However, despite the internal Pd–Pd distances, the Pd(dien)Br subunits do not appear to be entirely independent. Comparison of the bond lengths (Figure 5a) for two comparable Pd(dien) complexes,[31] $[Pd(dien)NO_2](NO_2)$ and $[Pd(Et_4dien)NO_2](NO_2)$, with those for the two complexes under consideration demonstrates that the geometries are essentially the same. The shortening of the Pd–N bond opposite the anionic ligand is presumably a result of the trans influence of the anion. The chelating angles in the five-membered rings are typical for systems of this kind.[32] In contrast, comparison of the mean planes through the three nitrogen atoms from the dien and the anion illustrates a marked distinction between the two types of complexes (Figure 5b). In both dinuclear complexes, the palladium atoms are displaced significantly out of the described plane toward each other, to the extent that the complexes may be viewed as quasi square pyramidal. Indeed, the basal angles for N(1)–Pd–N(3) and N(2)–Pd–Br in the $Pd_2([18]aneN_6)Br_2^{2+}$ cation are 167.1 and 168.7°, respectively, which are not very different from the values of 168.8 and 163.3° observed by Wieghardt et al.[33] for the five-coordinate 1,4,7-tris(2-pyridylmethyl)-1,4,7-triazacyclononane complex of Pd(II) and are consistent with the theoretical value for d^8 ions given by Hoffmann et al.[34]

In terms of the metal–metal vector in the dimeric complexes, the palladium atoms are closer together than the mean planes by 0.38 and 0.28 Å for the $Pd_2([18]aneN_6)Br_2^{2+}$ and $Pd_2([20]aneN_6)Br_2^{2+}$ cations, respectively. Since this distortion is not observable in the monomeric palladium dien complexes, it implies

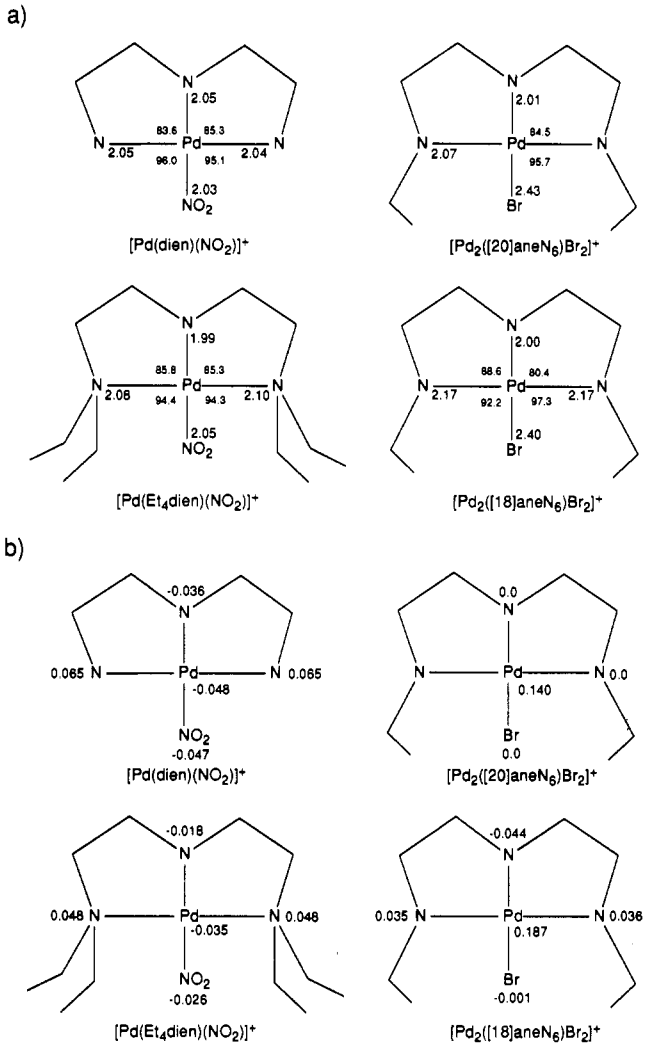

Figure 5. Comparison of coordination geometry for the structurally analogous species $Pd(dien)NO_2^+$, $Pd(Et_4dien)NO_2^+$, $Pd_2([18]aneN_6)Br_2^{2+}$, and $Pd_2([20]aneN_6)Br_2^{2+}$: (a) bond lengths (Å) and angles (deg) for atoms coordinated to the palladium ion; (b) perpendicular deviations from mean planes calculated for ligating atoms. The mean planes for $Pd(dien)NO_2^+$ and $Pd(Et_4dien)NO_2^+$ were calculated from data taken from ref 30.

that the two palladium ions, while not formally bonded, must be interacting to form some sort of favorable overlap at a shorter distance. A similar type of distortion has been observed by Piovesana et al.[35] for the dimeric palladium complex of dithioacetic acid. In that complex, the Pd–Pd distance is 0.14 Å shorter than that between the mean planes described by the coordinating atoms, giving a Pd–Pd distance of 2.754 Å. Piovesana et al. suggest this inward distortion reinforces the view of a strong Pd–Pd attractive interaction in their complex. A dinuclear rhodium(I) macrocyclic complex has been examined by Goedkin and coworkers,[36] and in that species, protonation leads to a slightly shorter Rh–Rh distance and oligomerization of the complex upon crystallization.

It should be noted that distortion of the N_3Br plane by involvement of the non-palladium atoms is viewed as unlikely. In the $Pd_2([18]aneN_6)Br_2^{2+}$ cation, hydrogen bonding between the bromide and the amine proton should draw the bromide closer to the nitrogen. This would result in an increase in the N(2)–Pd–Br angle and a decrease in the deviation of the palladium from the N_3Br plane. In the $Pd_2([20]aneN_6)Br_2^{2+}$ cation, all of the atoms in the N_3Br plane are well separated and are significantly

(28) Donohue, J. *The Structure of the Elements*; John Wiley and Sons: New York, 1974; p 216.
(29) Clegg, W.; Garner, C. D.; Al-Samman, M. H. *Inorg. Chem.* **1982**, *21*, 1897.
(30) Mann, K. R.; Gray, H. B. *Adv. Chem. Ser.* **1979**, *173*, 225.
(31) Bresciani, N.; Calligaris, M.; Randaccio, L.; Riceuuto, V.; Bellucio, U. *Inorg. Chim. Acta* **1975**, *14*, L17.
(32) (a) Wiesner, J. R.; Lingafelter, F. C. *Inorg. Chem.* **1966**, *5*, 1770. (b) Hori, F.; Matsumoto, K.; Ooi, S.; Kuroya, H. *Bull. Chem. Soc. Jpn.* **1977**, *50*, 138. (c) Toriumi, K.; Yamashita, M.; Ito, H.; Ito, T. *Acta Crystallogr., Sect. C* **1986**, *C42*, 963.
(33) Wieghardt, K.; Schöffmann, E.; Nuber, B.; Weiss, J. *Inorg. Chem.* **1986**, *25*, 4877.
(34) Rossi, A. R.; Hoffmann, R. *Inorg. Chem.* **1975**, *14*, 365.
(35) Pionesana, O.; Bellitto, C.; Flamini, A.; Zanazzi, P. F. *Inorg. Chem.* **1979**, *18*, 2258.
(36) Gordon, G. C.; DeHaven, P. W.; Weiss, M. C.; Goedkin, V. L. *J. Am. Chem. Soc.* **1978**, *100*, 1003.

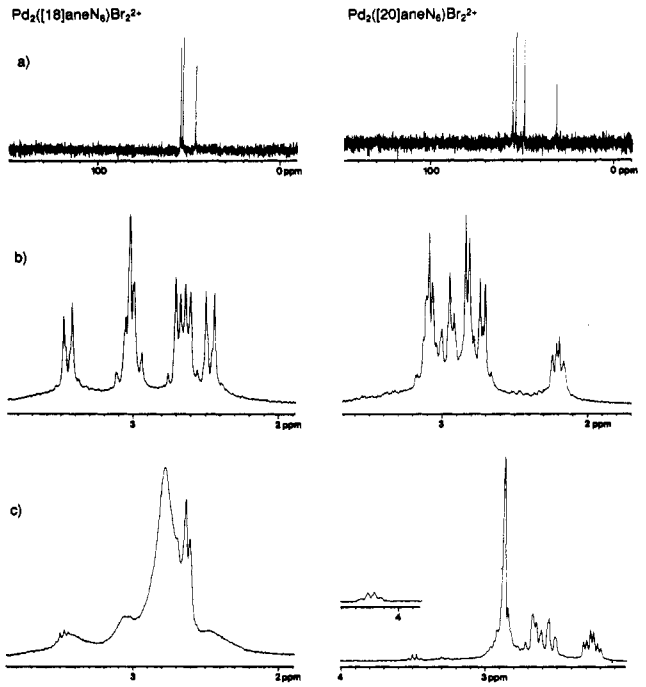

Figure 6. ^{13}C and ^{1}H NMR spectra for the $Pd_2([18]aneN_6)Br_2^{2+}$ and $Pd_2([20]aneN_6)Br_2^{2+}$ cations: (a) ^{13}C NMR spectra in D_2O; (b) ^{1}H NMR spectra in D_2O; (c) ^{1}H NMR spectra in D_2O after nonstoichiometric addition of NaOD.

beyond their collective van der Waals radii. In both cases, there is room for a closer approach of the ligand portion of the molecule. That this does not occur suggests that the palladium atoms are indeed attracted out of the plane by the adjacent metal atom, giving rise to the square-pyramidal geometry.

Nuclear Magnetic Resonance. The ^{1}H and ^{13}C NMR spectra for both $Pd_2([18]aneN_6)Br_2^{2+}$ and $Pd_2([20]aneN_6)Br_2^{2+}$ are shown in Figure 6 and indicate that the solution structure is essentially the same as the structure in the solid state. The ^{13}C NMR spectrum of $Pd_2([18]aneN_6)Br_2^{2+}$ exhibits only three resonances at 54.3, 53.0, and 46.0 ppm, due to the three types of carbon atoms within the molecule: the bridging methylenes and the two different carbons forming the chelating ring. The appearance of only three lines instead of lines for the six different carbons apparent in the crystal structure is a result of the vibrational motion of the molecules and the time averaging of the signals. The ^{13}C NMR spectrum of $Pd_2([20]aneN_6)Br_2^{2+}$ has three lines of equal intensity at 55.0, 53.3, and 48.7 ppm and a fourth line of approximately half-intensity at 31.1 ppm. From consideration of the crystalline structure and molecular symmetry, the upfield peak is the middle carbon of the 1,3-propanediyl bridge and the remaining resonances are similar to those observed for the $Pd_2([18]aneN_6)Br_2^{2+}$ cation.

The NMR spectra of these complexes suggest the absence of two dynamic processes that are conceivable for these complexes, namely, inversion of the trans structure to the cis for the $Pd_2([18]aneN_6)Br_2^{2+}$ cation (and vice versa for $Pd_2([20]aneN_6)Br_2^{2+}$) and any form of ring hopping around the equivalent nitrogen sites within the macrocycle. The latter process has recently been described for a bidentate $Pd([9]aneN_3)_2^{2+}$ complex.[37]

For $Pd_2([18]aneN_6)Br_2^{2+}$, the ^{1}H NMR spectrum exhibits superimposed AA'BB' and ABCD subspectra due the bridging and chelating ethylene chains, respectively. The overall intensity of the ABCD pattern is approximately twice that of the AA'BB' pattern as expected, and the simulated spectroscopic parameters are included in Table X. Of interest is the magnitude of J_{14}, the axial–axial coupling constant within the ABCD pattern, at 13.8 Hz. The Karplus equation[38] has been applied to a number of

Table X. ^{1}H NMR Parameters[a] for $Pd_2([18]aneN_6)Br_2^{2+}$ in D_2O

a. ABCD Subspectrum: Chelating Ethylenes

$\delta_1 = 3.05$	$\delta_b = 2.63$	$\delta_c = 2.70$	$\delta_d = 3.01$
$J_{ab} = -11.1$	$J_{ac} = 2.1$	$J_{ad} = 13.8$	
$J_{bc} = 1.3$	$J_{bd} = 1.7$		
$J_{cd} = -12.0$			

b. AA'BB' Subspectrum: Bridging Ethylenes

$\delta_a = \delta_{a'} = 3.46$	$\delta_b = \delta_{b'} = 2.48$
$J_{ab} = J_{a'b'} = -16.1$	$J_{aa'} = J_{bb'} = 7.9$
$J_{ab'} = J_{a'b} = 1.4$	

[a] All chemical shifts are in ppm; all coupling constants are in Hz.

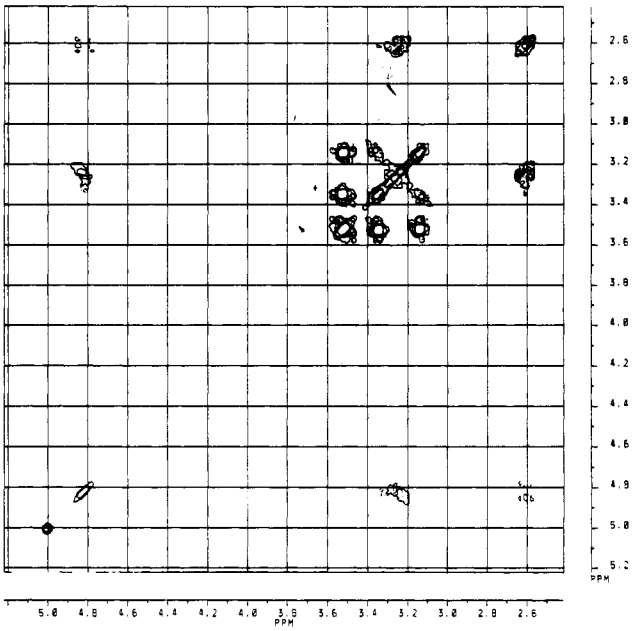

Figure 7. ^{1}H COSY NMR spectrum of $Pd_2([20]aneN_6)Br_2^{2+}$ obtained at 400 MHz in D_2O. The spectrum features two distinct subsets of resonances with the peaks at approximately 2.6, 3.25, and 4.8 ppm arising from the protons of the 1,3-propanediyl bridge while the peaks at approximately 3.15, 3.35, and 3.55 ppm are due to the protons of the chelating ethylene groups. All resonances are referenced to HOD at 5.0 ppm.

compounds containing five-membered chelate rings. The magnitude of the present coupling constant, when used in this equation, suggests that the protons are essentially 180° apart. Conformational features obtained from the solid-state structure suggest that this is indeed the case. In addition, the small coupling constants observed for the remaining atom pairs (except the geminal values) are in agreement with a high degree of rigidity in the ethylene group. This is a result of the constraints imposed by coordination of the palladium ion and enhances the view of these molecules as nonfluxional on the NMR time scale. In contrast, the AA'BB' pattern observed for the bridging ethylene groups is as expected and the coupling constants are more typical of the values observed for chelated ethylene units.[39]

A similar analysis of the ^{1}H NMR spectrum of the $Pd_2([20]aneN_6)Br_2^{2+}$ cation is not possible, due to the proximity and overlapping of the observed resonances, making assignment of individual peaks to a particular spectroscopic pattern difficult. Analysis of the spectra using conventional spin systems failed to provide a good computer simulation of the observed spectrum, suggesting unexplainable second-order effects. However, the 2-dimensional NMR spectrum (COSY) features two distinct subsets of resonances with the peaks at about 2.6, 3.25, and 4.8 ppm arising from the protons of the 1,3-propanediyl bridge while the peaks at about 3.15, 3.35, and 3.55 ppm are due to the protons of the chelating ethylene groups (Figure 7). Of particular interest

(37) Hunter, G.; McAuley, A.; Whitcombe, T. W. *Inorg. Chem.* **1988**, *27*, 2634.
(38) Karplus, M. *J. Am. Chem. Soc.* **1963**, *85*, 2870.
(39) Hawkins, C. J.; Palmer, J. A. *Coord. Chem. Rev.* **1982**, *44*, 1.

in this spectrum is the resonance at ≈4.8 ppm (relative to HOD at 5.0 ppm), which is due to one of the central protons of the 1,3-propanediyl bridge, as determined from coupling patterns and correlations observable in the COSY spectrum. This peak was not observable in the 250-MHz spectrum (Figure 6b) due to interference from the water resonance. This proton resonance is shifted ≈2.2 ppm downfield (deshielding) from its geminal partner at ≈2.6 ppm. It is suggested that this peak arises from the proton located within the cavity of the ligand between the two palladium ions, as illustrated in Figure 2. The direction of the shift is consistent with a paramagnetic effect, although of very small magnitude, resulting from a dipolar interaction with the electron density located between the metal centers. This is consistent with the view of some net metal–metal interaction in these complexes.

During the course of investigating the substitution reactions of these complexes, we observed that addition of OH^- produces a rapid, reversible loss of color in the solutions. In order to examine the products formed, ^1H NMR spectra (Figure 6c) were obtained of the D_2O solutions of the complexes after the nonstoichiometric addition of NaOD. The loss of coupling and of discernible peaks is readily apparent for both the [18]aneN$_6$ and [20]aneN$_6$ complexes. Although these spectra in basic media are not amenable to analysis, the presence of a dynamic process is clearly indicated. This is most likely a result of deprotonation of the nitrogen trans to the halide, resulting in a coordinated amide, which can facilitate the rapid fluctuation of the protons of the chelating ring. Deprotonation of this amine may also result in the dissociation of the coordinated halide. A consequence of this would then be the possible but unlikely inversion of the macrocyclic complexes to give the *cis*-Pd_2([18]aneN$_6$)Br_2^{2+} and *trans*-Pd_2([20]aneN$_6$)Br_2^{2+} cations. The ^1H NMR results, however, are not explicable by the simple substitution of OH^- for Br^- in the complex as is observed for other anions.

UV/Visible Spectroscopy and Substitution Kinetics. The UV/visible spectra of the Pd_2([18]aneN$_6$)Br_2^{2+} and Pd_2([20]aneN$_6$)Br_2^{2+} cations each exhibit a single peak at 355 nm (ϵ = 1500 M^{-1} cm^{-1}) and 351 nm (ϵ = 780 M^{-1} cm^{-1}), respectively, in aqueous solution. Similar spectra are obtained in DMSO (λ_{max} = 356 and 352 nm) with slightly lower extinction coefficients. Comparison of these values to the spectrum[40] of Pd(dien)Br^+ (λ_{max} = 342 nm, ϵ = 450 M^{-1} cm^{-1}) suggests that the Pd_2([20]aneN$_6$)Br_2^{2+} cation behaves as two "Pd(dien)Br^{+}" subunits with an effective extinction coefficient of ≈390 M^{-1} cm^{-1} for each Pd(II). However, for Pd_2([18]aneN$_6$)Br_2^{2+}, the effective extinction coefficient is ≈750 M^{-1} cm^{-1}, more than twice the value for Pd(dien)Br^+ and more typical of the values observed[41] for Pd(Et$_4$dien)Br^+ (λ_{max} = 358 nm, ϵ = 690 M^{-1} cm^{-1}).[43] This is an interesting comparison, since the crystal structures[31] of both Pd(dien)$(NO_2)^+$ and Pd(Et$_4$dien)$(NO_2)^+$ (and, presumably, the corresponding bromide complexes) have planar palladium ions with essentially the same coordination geometry as those exhibited by the dimers (Figure 5a). It appears that the pyramidalization of the palladium ions in the dimeric complexes has not altered significantly the relative energies of the observed transitions.

Addition of various anions (e.g. SCN^-) or neutral molecules (e.g. pyridine) results in the substitution of the coordinated bromide ion. Hydroxide ion reacts moderately rapidly with Pd_2([20]aneN$_6$)Br_2^{2+} ($t_{1/2}$ ≈ 30 s) and somewhat more slowly with Pd_2([18]aneN$_6$)Br_2^{2+} ($t_{1/2}$ ≈ 150 s) to give essentially colorless solutions. Reacidification of the solution regenerates the initial spectrum, suggesting a reversible equilibrium for the deprotonation rather than a decomposition reaction. These observations are consistent with the NMR spectroscopy of these complexes (vide supra).

The rate of bromide substitution by I^- for the two cations has been measured in aqueous media (pH ≈ 7, T = 31 °C). For both species, the reaction was monitored under pseudo-first-order conditions (iodide in excess) at λ_{max} for the corresponding iodo salt (Pd_2([18]aneN$_6$)I_2^{2+}, 382 nm, ϵ = 2300 M^{-1} cm^{-1}; Pd_2([20]aneN$_6$)I_2^{2+}, 381 nm, ϵ = 1020 M^{-1} cm^{-1}). First-order kinetics were observed in both instances. For the Pd_2([20]aneN$_6$)Br_2^{2+} complex ion, the observed rate constant was dependent upon the iodide concentration with a slope of (3.9 ± 0.6) × 10^{-2} M^{-1} s^{-1} and an intercept of (3.4 ± 0.1) × 10^{-3} s^{-1}. A two-term rate law is observed generally for the substitution reactions of Pd(dien)X^+ and N-alkylated Pd(dien)X complexes[40] and has been rationalized by postulating a solvolysis pathway in the mechanistic scheme. A similar mechanism may thus be written for the Pd_2([20]aneN$_6$)Br_2^{2+} cation:

$$Pd_2([20]aneN_6)Br_2^{2+} + H_2O \xrightarrow{k_1} Pd_2([20]aneN_6)Br(OH_2)^{3+} + Br^-$$

$$+I \downarrow \text{fast}$$

$$Pd_2([20]aneN_6)Br_2^{2+} + I^- \xrightarrow{k_2} Pd_2([20]aneN_6)Br(I)^{2+} + Br^-$$

where k_1 is for the solvolysis pathway and k_2 represents the direct substitution reaction. The values obtained for Pd_2([20]aneN$_6$)Br_2^{2+} are typical of those obtained[42] for N-alkylated Pd(dien)X^+ complexes with a moderate amount of steric hindrance (e.g. Pd(Me$_5$dien)X^+) which display similar nucleophile dependent and independent pathways. This suggests that each Pd center undergoes independent substitution at a similar rate.

Substitution reactions for square-planar compounds are generally postulated to proceed through an associative mechanism to give, initially, a square-pyramidal and then a trigonal-bipyramidal transition state.[41] Hindered N-alkylated Pd(dien)X^+ complexes have been described, not as square-planar species, but as pseudo-octahedral ions owing to the steric bulk of the alkyl groups blocking access to the axial sites. A change in mechanistic pathway from an associative to a dissociative reaction has been postulated.[42] The dimeric complexes do not possess such bulky groups blocking both axial sites on the palladium ion, but the pseudo-square-pyramidal configuration "buries" the palladium within the ligand.

For the Pd_2([18]aneN$_6$)Br_2^{2+} cation, under conditions of greater than 20-fold [I^-] excess, the rate of substitution is independent of the iodide concentration. However, there is evidence for two consecutive [I^-]-independent steps with rate constants k_a = (8.0 ± 0.3) × 10^{-4} s^{-1} and k_b = (6.4 ± 0.5) × 10^{-5} s^{-1}. A nucleophile-independent pathway implies a dissociative mechanism wherein the loss of the bromide produces a coordinatively unsaturated species. Similar kinetics have been observed for more sterically hindered monomeric Pd(II) complexes (e.g. Pd(Et$_4$Medien)X^+) with rate constants[41] similar in magnitude to those observed for the dimeric species. The comparison between rate constants and mechanistic pathways for the two dimeric palladium complexes mirrors the relative changes in their UV/visible spectra.

The substitution of thiocyanate into the Pd_2([18]aneN$_6$)Br_2^{2+} cation has also been examined. Again, the observed reaction profiles were biphasic. However, in this case there is evidence for "saturation" kinetics, where the substitution rate increases to a limiting value. The initial data were analyzed by using the mechanism

$$Pd_2([18]aneN_6)Br_2^{2+} \underset{k_{-1}}{\overset{k_1}{\rightleftharpoons}} Pd_2([18]aneN_6)Br^{3+} + Br^-$$

$$Pd_2([18]aneN_6)Br^{3+} + SCN^- \xrightarrow{k_2} Pd_2([18]aneN_6)Br(SCN)$$

resulting in the rate law

$$k_{obs} = \frac{k_1 k_2 [SCN^-]}{k_{-1}[Br^-] + k_2[SCN^-]}$$

At high thiocyanate concentrations, k_2[SCN^-] ≫ k_{-1}[Br^-], so that k_{obs} = k_1 ($=k_a$). The value obtained for k_1 by using a nonlinear

(40) Palmer, D. A.; Kelm, H. *Inorg. Chim. Acta* **1975**, *14*, L27.
(41) Baddley, W. H.; Basolo, F. *J. Am. Chem. Soc.* **1966**, *88*, 2944.
(42) (a) Kotowski, M.; van Eldik, R. *Inorg. Chem.* **1986**, *25*, 3896. (b) Breet, E. L. J.; van Eldik, R.; Kelm, H. *Polyhedron* **1983**, *2*, 1181.
(43) Gray, H. B.; Olcott, R. J. *Inorg. Chem.* **1962**, *1*, 481.
(44) Atwood, J. D. *Inorganic and Organometallic Reaction Mechanisms*; Brooks/Cole: Monterey, CA, 1985.

least-squares analysis is (8.3 ± 0.2) × 10^{-4} s^{-1}, which is in agreement with the value obtained for iodide, providing further evidence for a dissociative mechanism. The second reaction is independent of the nucleophile concentration with a rate constant of (1.4 ± 0.1) × 10^{-4} s^{-1}.

The concentration profile does not eliminate an associative pathway for the above equilibria involving aquation of the palladium center concurrent with loss of the halide. However, owing to the constrained "square-pyramidal" geometry of the Pd centers, it is viewed as unlikely that such an association would be favored. In view of the similarity of the k_a values in both the I^- and SCN^- substitution reactions, we postulate a rate-limiting dissociation of the bromide. It is possible that the presence of the second Pd acting as a "fifth" ligand provides the necessary stabilization of the transition state which would no longer be akin to the three-coordinate ion that must be formed in the monomeric reaction pathway.

Acknowledgment. We thank the NSERC and the University of Victoria for financial support. T.W.W. acknowledges the receipt of an NSERC Postgraduate Scholarship. We also wish to acknowledge the contribution of Mrs. K. Beveridge.

Supplementary Material Available: Tables S1-S16, containing crystallographic parameters, bond lengths, bond angles, atomic coordinates, temperature parameters, intermolecular distances, and mean planes and deviations for $Pd_2([18]aneN_6)Br_2 \cdot 4H_2O$ and $Pd_2([20]aneN_6)Br_2 \cdot H_2O$, and a contour plot of the 2-dimensional COSY spectrum for $Pd_2([20]aneN_6)Br_2^{2+}$ in D_2O (12 pages); Tables S17 and S18, listing structure factors for $Pd_2([18]aneN_6)Br_2 \cdot 4H_2O$ and $Pd_2([20]aneN_6)Br_2 \cdot H_2O$ (12 pages). Ordering information is given on any current masthead page.

Contribution from the Department of Chemistry,
Case Western Reserve University, Cleveland, Ohio 44106

Divalent Metal Ion Catalyzed Hydrolysis of Picolinanilides[1]

K. Veera Reddy, Alan R. Jacobson, John I. Kung, and Lawrence M. Sayre*

Received August 3, 1990

The hydrolysis of *N*-methylpicolinanilides bearing electron-withdrawing substituents (4-nitro, 2,4-dinitro, and 5-chloro-2-nitro) was studied as a function of pH at 40.0 °C in ethanol-water (1:2) in the absence and presence of divalent metal ions, in particular Cu(II). Plots of log *k* vs pH for *uncatalyzed* hydrolysis were linear with unit slope over the pH range 9-12, permitting the calculation of bimolecular k_{OH} values for this region. Plots of log *k* vs pH in the presence of various concentrations of Cu$(NO_3)_2$-bpy (1:1) increased linearly (slope = 1) over the pH range 5.0-6.2, plateaued over the pH region 7-9, and increased again at higher pH as the uncatalyzed reaction came to prominence. Catalysis by Cu(II) in the absence of bpy (for the 4-nitroanilide) could be followed only below pH 6, but log *k* increased linearly (slope = 1) in the pH range 4-6. The unit slope behavior at low pH for both the Cu^{II}(bpy)- and Cu^{II}-catalyzed reactions was interpreted in terms of Cu(II) catalysis of hydroxide-mediated hydrolysis. Second-order k_{OH}(Cu) values could be calculated from the unit slopes, which, when compared to the uncatalyzed k_{OH} values, indicate catalytic rate enhancements of 10^4-10^5 induced by 10 mM Cu^{II}(bpy). Saturation effects were seen for the 4-nitroanilide at high [Cu(II)] (±bpy), permitting an extrapolation to the maximum catalytic effect in these cases ((1-8) × 10^6). These catalytic factors are discussed in comparison to related systems studied by other workers.

Introduction

Despite the many studies carried out to elucidate the nature of metal ion catalysis of amide hydrolysis, the criteria that must be met for observing large catalytic rate enhancements and the mechanisms of the processes involved remain incompletely understood. In fact, it was believed at one time that hydrolysis of *simple* amides is not subject to large *catalytic*[2] effects of metal ions, in contrast to the situation with esters, where rate enhancements as large as 10^8 were observed.[3] This dichotomy was alleged to be a consequence of the fact that whereas ester hydrolysis follows a rate-limiting tetrahedral intermediate (TI) formation mechanism, amide hydrolysis generally follows a rate-limiting TI breakdown mechanism at pH ~ 7 due to the absence of a good leaving group.[4] In this way, the much greater rate accelerating effect of metal ions on ester hydrolysis than on amide hydrolysis might be ascribed to the expectation that a metal ion would have a greater catalytic effect on TI formation than on TI breakdown. According to this interpretation, the use of special amides where leaving group ability could be made as good as that of alkoxide should result in a switch to a rate-limiting TI formation mechanism, and pronounced metal ion catalysis should then be observed.

One straightforward approach to a systematic investigation of leaving group ability would be to employ substituted anilides, since the basic hydrolysis of *N*-alkyl anilides containing at least a *p*-nitro substituent is known to follow a rate-limiting TI formation pathway.[5] We chose *N*-methylpicolinanilides, where the pyridine N provides a coordination site for metal ions in a way that would encourage a carbonyl-activation and/or "metal hydroxide" mechanism and where the *N*-methyl group eliminated the chance of chelation-promoted NH deprotonation, which would generate a hydrolytically inert "amido" complex.[6] We chose to include 2,4-dinitro and 5-chloro-2-nitro substitution patterns since *o*-nitro has been found not only to retard TI formation as a consequence of steric inhibition of resonance but also to sterically accelerate TI breakdown, thus further assuring a rate-limiting TI formation mechanism.[7]

During our initial efforts,[8] Fife and Przystas published a study based on essentially the same premise, employing *N*-picolinylimidazoles.[9] These workers observed rate-enhancement factors

(1) This study was presented in preliminary form: Reddy, K. V.; Sayre, L. M. *Abstracts of Papers*, 199th National Meeting of the American Chemical Society, Boston, April 22-27, 1990; American Chemical Society: Washington, DC, 1990; INOR 189.

(2) Large rate enhancements have been seen for Co(III) systems (see: Sutton, P. A.; Buckingham, D. A. *Acc. Chem. Res.* **1987**, *20*, 357 and references cited therein), though the metal in these cases is stoichiometrically bound to the product, so that these reactions were considered to represent a metal ion *promoted* rather than metal ion catalyzed process.

(3) (a) Hay, R. W.; Morris, P. J. *Met. Ions Biol. Syst.* **1976**, *5*, 173. (b) Martell, A. E. *Met. Ions Biol. Syst.* **1973**, *2*, 207. (c) Hay, R. W.; Clark, C. R. *J. Chem. Soc., Dalton Trans.* **1977**, 1866, 1993. (d) Fife, T. H.; Przystas, T. J.; Squillacote, V. L. *J. Am. Chem. Soc.* **1979**, *101*, 3017.

(4) (a) DeWolfe, R. H.; Newcomb, R. C. *J. Org. Chem.* **1971**, *36*, 3870. (b) Pollack, R. M.; Bender, M. L. *J. Am. Chem. Soc.* **1970**, *92*, 7190. (c) Kershner, L. D.; Schowen, R. L. *J. Am. Chem. Soc.* **1971**, *93*, 2014.

(5) Broxton, T. J. *Aust. J. Chem.* **1984**, *37*, 2005. Broxton, T. J.; Deady, L. W. *J. Org. Chem.* **1975**, *40*, 2906.

(6) (a) Grant, I. J.; Hay, R. W. *Aust. J. Chem.* **1965**, *18*, 1189. (b) Conley, H. L., Jr.; Martin, R. B. *J. Phys. Chem.* **1965**, *69*, 2914.

(7) (a) Skarzewski, J.; Aoki, M.; Sekiguchi, S. *J. Org. Chem.* **1982**, *47*, 1764. (b) Kajima, A.; Sekiguchi, S. *Bull. Chem. Soc. Jpn.* **1987**, *60*, 3597.

(8) Sayre, L. M.; Jacobson, A. R. *Abstracts of Papers*, 191st National Meeting of the American Chemical Society, New York, April 14-18, 1986; American Chemical Society: Washington, DC, 1986; INOR 233.

(9) Fife, T. H.; Przystas, T. J. *J. Am. Chem. Soc.* **1986**, *108*, 4631.

0020-1669/91/1330-3520$02.50/0